Pure

Syddansk Universitet

# Neutron reflectivity of supported membranes incorporating terminally anchored polymers: Protrusions vs. blisters

Fragneto, Giovanna; Halperin, Avraham; Klösgen, Beate; Sferrazza, Michele

*Published in:*
European Physical Journal E. Soft Matter

*DOI:*
10.1140/epje/i2013-13003-6

*Publication date:*
2013

*Citation for pulished version (APA):*
Fragneto, G., Halperin, A., Klösgen-Buchkremer, B. M., & Sferrazza, M. (2013). Neutron reflectivity of supported membranes incorporating terminally anchored polymers: Protrusions vs. blisters. European Physical Journal E. Soft Matter, 36(1), 1-7. DOI: 10.1140/epje/i2013-13003-6

**General rights**
Copyright and moral rights for the publications made accessible in the public portal are retained by the authors and/or other copyright owners and it is a condition of accessing publications that users recognise and abide by the legal requirements associated with these rights.

- Users may download and print one copy of any publication from the public portal for the purpose of private study or research.
- You may not further distribute the material or use it for any profit-making activity or commercial gain
- You may freely distribute the URL identifying the publication in the public portal ?

**Take down policy**
If you believe that this document breaches copyright please contact us providing details, and we will remove access to the work immediately and investigate your claim.

Download date: 23. Feb. 2018

Eur. Phys. J. E (2013) **36**: 3
DOI 10.1140/epje/i2013-13003-6

THE EUROPEAN PHYSICAL JOURNAL E

Regular Article

# Neutron reflectivity of supported membranes incorporating terminally anchored polymers: Protrusions vs. blisters

G. Fragneto[1,a], A. Halperin[2], B. Klösgen[3], and M. Sferrazza[4]

[1] Institute Max von Laue - Paul Langevin, 6 rue Jules Horowitz, BP 156, 38042 Grenoble, France
[2] Université de Grenoble 1/CNRS, LIPhy UMR 5588, BP 87, 38041 Grenoble, France
[3] Department of Physics, Chemistry and Pharmacy, and MEMPHYS, Center for Biomembrane Physics, University of Southern Denmark, Campusvej 55, 5230 Odense M, Denmark
[4] Département de Physique, Faculté des Sciences, Université Libre de Bruxelles, Boulevard du Triomphe, 1050 Bruxelles, Belgium

Received 16 September 2012 and Received in final form 28 November 2012
Published online: 17 January 2013 – © EDP Sciences / Società Italiana di Fisica / Springer-Verlag 2013

**Abstract.** The effect of terminally anchored chains on the structure of lipid bilayers adsorbed at the solid/water interface was characterized by neutron reflectivity. In the studied system, the inner leaflet, closer to the substrate, consisted of head-deuterated 1,2-distearoyl-sn-glycero-3-phosphorylcholine (DSPC) and the outer leaflet comprised a mixture of DSPC and polyethylene glycol (PEG) functionalized 1,2-distearoyl-sn-glycero-3-phosphoethanolamine. The DSPC headgroups were deuterated to enhance sensitivity and demarcate the bilayer/water interface. The effect on the inner and outer headgroup layers was characterized by $w_{1/2}$, the width at half-height of the scattering length density profile. The inner headgroup layer was essentially unperturbed while $w_{1/2}$ of the outer layer increased significantly. This suggests that the anchored PEG chains give rise to headgroup protrusions rather than to blister-like membrane deformations.

## 1 Introduction

Lipid membranes bearing terminally anchored polymers attract interest because similar motifs occur in living cells [1] and because of their utility in drug delivery [2] and their distinctive phenomenology [3]. Theory efforts in this area involved two approaches, both considering the consequences of the chain entropy loss due to anchoring its terminus at an impenetrable surface [4]. In one approach the membrane was modeled as a flexible uniform surface characterized by a bending modulus [5–9]. Within this continuum description the membrane surrounding the anchoring site accommodates the chain by bending away from it. The height profile of the polymer-bearing membrane reflects the interplay between the entropy loss of the polymer and the deformation penalty of the membrane. The analysis yields the shape of the polymer-bearing membrane, the effect on its spontaneous curvature as well as information on the interactions between the grafted chains. The second, molecular approach focused on the effect of grafted polymers on unimodal protrusions of functionalized lipids, *i.e.* fluctuations in the height of lipid headgroups that incur a free-energy penalty due to the exposure of the hydrophobic tails to water [10–12]. Here the interplay between the hydrophobic penalty and the loss of chain entropy stabilizes the protrusions of polymer-bearing headgroups thus rendering them equilibrium structures characterized by an average head group height, $z_p^{\rm eq} > 0$ [13] (fig. 1). Note that this simple analysis overlooks cooperative protrusions involving a number of lipids, an effect that enhances the protrusions but does not change the scaling behavior of the protrusion height [14, 15]. This second approach was motivated by observations concerning secretory phospholipase $A_2$ (sPLA$_2$), an interfacially active enzyme that selectively hydrolyzes lipids incorporated into membranes [16, 17], in particular its enhanced activity when the substrate membrane incorporates lipids bearing the water-soluble polymer poly(ethylene glycol) (PEG) [13]. The model hypothesized that the mechanism of hydrolysis by sPLA$_2$ involves protrusions allowing the lipid headgroup to access the active site of the enzyme. Within this picture, the anchored PEG chains stabilize the protrusions thus increasing the enzymatic activity.

The experimental support for the occurrence of PEG stabilized protrusions in *membranes* is currently indirect, being based on the ability of this picture to rationalize observations regarding sPLA$_2$ [18]. Early experimental evidence concerning polymer-induced protrusions was obtained in three studies involving lipid *monolayers*. Neutron reflectometry (NR) [19] as well as X-ray reflectometry and grazing incidence diffraction [20] were used to probe mixed monolayers of lipids and PEG-lipids at water-air interfaces. Both hydrogenated and deuterated lipid tails

[a] e-mail: fragneto@ill.eu

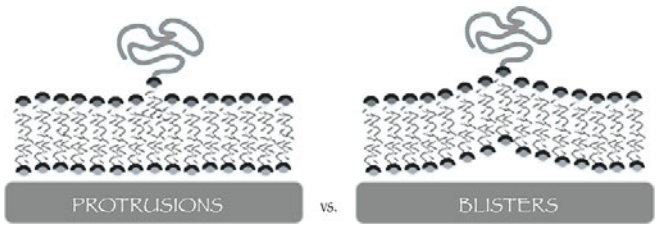


**Fig. 1.** Schematic view of unimodal protrusion *vs.* blister.

were employed in the NR experiment [19]. Another study investigated similar mixed monolayers on solid substrates hydrophobized by chemically grafted and thus immobile monolayers of octadecyltrichlorosilane (OTS) [21]. The experiments were carried out at a single temperature $T = 21\,^{\circ}\mathrm{C}$ and the polymerization degree of the PEG chain in PEG-lipids was $N = 45$. In every case the roughness of the headgroup layer increased with the mole fraction of PEG-lipids and the results were interpreted in terms of non-equilibrium protrusions rather than PEG-stabilized ones. However, as we shall discuss, monolayer experiments do not allow to distinguish between the predictions of the continuum and protrusions pictures. In contrast, for supported lipid bilayers the two pictures differ in their predictions concerning the effective thickness of the two headgroups layers. In NR experiments these models are distinguishable via $w_{1/2}$, the width at half-height of the scattering length density profiles of the *two* deuterated headgroup layers. With this in mind, we extended the early monolayer experiments and utilized NR to study the effect of grafted chains on supported lipid membranes with deuterated headgroups. In particular we investigated asymmetric lipid bilayers where the inner leaflet consisted of non-functionalized lipid while the exterior one comprised a binary mixture of PEG lipids and and non-functionalized lipids. Furthermore we utilized two different PEG-lipids incorporating PEG chains comprising of $N = 16$ (MW = 750 g/mol) and $N = 45$ (MW = 2000 g/mol) monomers. Measurements were carried out at four different temperatures $T = 298$, 333.5, 344.5, 352.5 K. For both $N$ values the mole fraction of PEG lipids $f$ was chosen to achieve two regimes: non-overlapping mushrooms and brushes of weakly crowded PEG chains $f = 1.3\%$, 9% for $N = 16$ and $f = 0.35\%$, 3.5% for $N = 45$. The inner membrane leaflet consisted of 1,2-distearoyl-sn-glycero-3-phosphorylcholine (DSPC) and the outer one comprised a mixture of DSPC and polyethylene glycol functionalized 1,2-distearoyl-sn-glycero-3-phosphoethanolamine (DSPE-PEG). The DSPC incorporated deuterated headgroups (molecular formula $C_{44}H_{75}NO_8PD_{13}$) and is denoted in the following by d-DSPC. In our study the $Si/SiO_2$ supported bilayers were separated from the substrate by a 5 Å thick water layer allowing for limited membrane deformation. For this system the molecular and the continuum pictures suggest two scenarios leading to different predictions concerning $w_{1/2}$ of the headgroup layers: a) Polymer stabilized protrusions [13] selectively enhancing $w_{1/2}$ of the outer headgroup layer, b) "Blisters" of fluid trapped between the substrate and the polymer-induced membrane deformation [8] and leading to similar $w_{1/2}$ for both inner and outer headgroup layers. For our particular system, the results favor protrusions over blisters because the grafted polymers give rise to an increase in $w_{1/2}$ of the outer headgroup layer with negligible effect on the inner leaflet.

## 2 Summary of theoretical scenarios

Two scenarios of polymer-induced membrane effects are considered in our subsequent discussion. In the first [8] the membrane is viewed as a deformable sheet and the grafted chains give rise to fluid filled "blisters" where the membrane curves away from the substrate thus reducing the entropy loss of the polymer. The analysis balances the bending energy of the deformed membrane, the configurational entropy of the anchored polymer and the adhesion energy associated with the membrane-substrate contact. For the case of a rigid membrane and/or strong adhesion it predicts largely conical blisters with height

$$z^{\mathrm{eq}}_{\mathrm{blister}} \sim \frac{(k_B T)^2}{\kappa^{3/2} \Gamma_m^{1/2}} \tag{1}$$

and radius

$$R_{\mathrm{blister}} \sim \frac{k_B T}{\kappa^{1/2} \Gamma_m^{1/2}}\,, \tag{2}$$

where $\Gamma_m/2$ is the membrane-substrate adhesion energy per unit area, $\kappa$ is the bending rigidity, $k_B$ is the Boltzmann constant and $T$ is the temperature. Neither $z^{\mathrm{eq}}_{\mathrm{blister}}$ nor $R_{\mathrm{blister}}$ depend on the polymerization degree of the polymer, $N$. In qualitative terms the blisters involve the deformation of the lipid bilayer viewed as a uniform sheet. Consequently the model predicts that the inner and outer headgroups layers will exhibit similar behavior. The second scenario concerns the stabilization of headgroup protrusions [13,18]. The effect of the polymer on single headgroup protrusion of the lipid anchoring the chain is determined by balancing the hydrophobic penalty of the exposed hydrocarbon tail with the entropy loss of the polymer. A lipid with its headgroup at height $z$ above a planar surface of the surrounding headgroups incurs a penalty $\alpha z$, where $\alpha$ is the free energy penalty per unit length due to the exposure of the protruding hydrocarbon tail to water [10–12]. For an isolated Gaussian chain terminally anchored at height $z$ above an impenetrable planar surface, the number of chain configurations, $Z_a(z)$, is reduced by a factor of $Z_a(z)/Z_0 = \mathrm{erf}(z/2R_0)$ with respect to $Z_0$, the number of available configurations to a free ideal chain having a radius $R_0 \approx N^{1/2} a$, where $a$ is the monomer size [4]. When $z \ll R_0$, the case of interest, $Z_a(z)/Z_0 \approx z/\pi^{1/2} R_0$ and the corresponding loss of entropy is $\Delta S = k_B \ln[Z_a(z)/Z_0] = k_B \ln(z/R_0) + \mathrm{const.}$ Minimization of the the excess free energy of the protrusions of polymer-bearing lipids, $\Delta F = -k_B T \ln(z/R_0) + \alpha z$ yields an equilibrium height

$$z_p^{\mathrm{eq}} = \frac{k_B T}{\alpha} > 0 \tag{3}$$

identical in value to the average height of protrusions of non-functionalized lipids, $\bar{z}_{\mathrm{free}} = z_p^{\mathrm{eq}}$, whose equilibrium

height is $z_{\rm free}^{\rm eq} = 0$. In the discussion of isolated grafted chains, "mushrooms", $Z_a(z)$ accounts for the total number of available configurations, irrespective of the height of the free end. A slight modification is necessary when considering brushes where $Z_a(z)$ is replaced by $Z_a(z, z_N)$, the number of configurations per unit length when the free end is in an infinitesimal layer at altitude $z_N$. Within the framework of the Alexander model, where all free ends are localized at the brush edge at height $H$, this leads again to $z_p^{\rm eq}$ as given by (3) (appendix A).

The protrusion and blister models exhibit certain common features. Both $z_p^{\rm eq}$ and $z_{\rm blister}^{\rm eq}$ are independent of $N$. The two pictures also suggest that the effective thickness increases with the PEG-lipid mole fraction, $f$. Crudely, one may relate the effective thickness to the $f$ weighted height $\langle z\rangle_f = (1-f)z_{\rm free}^{\rm eq} + f z_i^{\rm eq}$ where $z_{\rm free}^{\rm eq} = 0$ denotes the equilibrium height of non-functionalized lipids and $z_i^{\rm eq} > 0$ is the equilibrium height of the protrusions ($i = p$) or the blisters ($i =$ blister) as given by (1) or (3). However, the two descriptions vary qualitatively in their predictions regarding the inner and outer headgroup layers of an asymmetric lipid membrane. Within the blister picture the two headgroup layers deform in tandem leading to identical increase in their NR $w_{1/2}$. In contrast, the protrusion picture suggests that only the $w_{1/2}$ of the outer, PEG-bearing, headgroup layer increases with $f$.

To conclude this section, it is useful to outline the interpretation used by Majewski *et al.* [19] and clarify its relationship to the models described earlier. Their approach combines two ingredients. First the protrusions are considered as fluctuations for both simple and PEG lipids. Following Annianson [11,12] the head group density at altitude $z$ is thus assumed to be given by $c(z) = c(0)\exp(-\alpha z/k_BT)$ where the maximal $z$, $z_{\rm max}$ is the length of the extended tail. The *average* height of a headgroup, allowing for fluctuations is $\bar{z} = k_BT/\alpha$ while the equilibrium height is $z^{\rm eq} = 0$. The second ingredient concerns $\alpha$. It is argued that $c(z_{\rm max})$ is comparable to the critical micelle concentration (cmc) thus suggesting approximating $\alpha$ by $\alpha_{\rm cmc} = -(k_BT/z_{\rm max})\ln({\rm cmc})$. Since the cmc of DSPE-EO$_{45}$ is $\approx 5$ orders of magnitude higher than that of DSPE, the corresponding $\alpha_{\rm cmc}$ values differ being $\alpha_{\rm cmc}({\rm DSPE})/k_BT = 1.1\,{\rm Å}^{-1}$ and $\alpha_{\rm cmc}({\rm DSPE\text{-}EO_{45}})/k_BT = 0.6\,{\rm Å}^{-1}$. In turn, this suggests that $\bar{z}_{\rm DSPE\text{-}EO_{45}} > \bar{z}_{\rm DSPE}$ and attributes the roughness to the $N$ dependence of $\alpha_{\rm cmc}$. Note, however, that $\alpha_{\rm cmc}$ thus obtained reflects not only the hydrophobic contribution but also a brush penalty due to the dense PEG corona of the DSPE-EO$_{45}$ micelles. Within our treatment $\alpha$ is independent of $N$ and the enhanced roughness arises because of the polymer-induced stabilization of the protrusions of PEG lipids.

## 3 Experimental section

The preparation of freely floating bilayers on the solid substrate [22] utilized a combination of the Langmuir-Blodgett and the Langmuir-Schaefer methods. This procedure is already widely used for membrane deposition

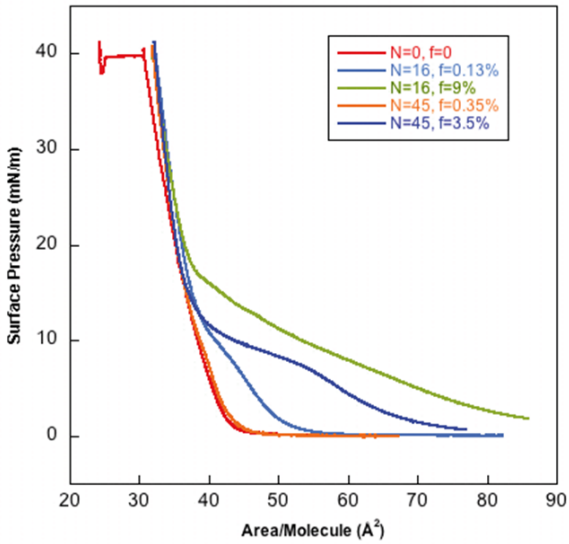


**Fig. 2.** The compression isotherms depicting the surface pressure *vs.* the mean area per lipid at 23 °C for the pure and mixed monolayers as specified in the inset.

on various substrates, such as $SiO_2$, glass or mica. In the present study, the substrates were crystalline silicon wafers of dimension 5 cm × 5 cm × 1 cm, orientation (111) and polished on one large surface to a roughness less then 3 Å. Before lipid deposition the Si substrates were carefully cleaned by ultra-sonication in successive baths of chloroform, acetone, and ethanol, followed by thorough rinsing in Millipore water. After drying in a soft nitrogen stream they were exposed to ozone plasma to obtain hydrophilic wafers free of organic remnants. Throughout both deposition steps, the interfacial lipid layer was kept at a constant surface pressure of 40 mN/m. Figure 2 shows the adsorption isotherms of the different lipid compositions as acquired immediately before deposition on the substrate. At surface pressures higher than 20 mN/m the isotherms reflect interactions between the lipids. Polymer effects are evident at lower lipid densities with shorter length PEG ($N = 16$) presenting more pronounced effects than the longer ones ($N = 45$). The interpretation of the monolayer behaviour and isotherms' shape is beyond the scope of this work. The deposition at constant pressure was carried out at 40 mn/m, where lipids are closely packed and the repulsive interactions dominate the isotherms.

The deposition of the inner monolayer of the adsorbed bilayer was performed by slowly pulling out of the water the substrate, previously immersed in the well of a Langmuir trough, while keeping the deposited monolayer at constant surface pressure. Next, the surface of the Langmuir trough was thoroughly cleaned, a new monolayer was spread and compressed, the substrate installed parallel to the water surface and slowly pulled down to contact the surface and form the bilayer on the substrate. All lipids were purchased from Avanti Polar Lipids (Lancaster, Alabama, US) and used as delivered. The bilayers prepared by this procedure formed uniform films suitable for neutron experiments. The mole fractions of

PEG lipids, $f$, were: $f = 1.3\%$, 9% for $N = 16$ and $f = 0.35\%$, 3.5% for $N = 45$. The Flory radii of the free PEG chains, $R_F = aN^{0.6}$ assuming a monomer size $a = 4\,\text{Å}$ are respectively 21 Å and 39 Å for the $N = 16$ and $N = 45$ chains. We have used $a = 4\,\text{Å}$ since the measured PEG density of $1.13\,\text{g/cm}^3$ and the scattering length density $0.64 \times 10^{-6}\,\text{Å}^{-2}$ [29] are both consistent with a monomer volume of $a^3 \approx 64\,\text{Å}^3$. The $R_F$ values, together with the area per PEG chain $\Sigma$, specify the chain crowding. In turn, $\Sigma$ is determined from the area per headgroup maintained during the Langmuir deposition and $f$. For $N = 45$ we obtain $\Sigma = 700\,\text{Å}^2$ for $f = 3.5\%$ and $\Sigma = 9600\,\text{Å}^2$ for $f = 0.35\%$, while for $N = 16$ we find $\Sigma = 404\,\text{Å}^2$ for $f = 9\%$ and $\Sigma = 3123\,\text{Å}^2$ for $f = 1.3\%$. This suggests that the $N = 45$, $f = 3.5\%$ and $N = 16$, $f = 9\%$ samples are in the brush regime ($\Sigma < R_F^2$), while the $N = 45$, $f = 0.35\%$ and the $N = 16$, $f = 1.3\%$ samples are in the mushroom regime ($\Sigma > R_F^2$). After the bilayer deposition, the substrates were tightly mounted to a small Teflon trough filled with 5 ml of water that served to hold the bulk liquid subphase facing the lipid bilayers. Luer-lock inlets allowed exchange of the aqueous filling by use of syringes such that the contrast of the lipid/water interface could be modified by replacement of the water phase during the experiments. Further details of the solid-liquid cell used for the neutron reflectivity experiment are described in [23]. Due to the difference in neutron scattering length between hydrogen and deuterium, standard techniques of isotopic labeling and contrast matching can be used to separate and amplify the contributions from the various components of the lipid bilayers, and to modulate contrast among different layers within multilayer samples. We have chosen to enhance the signal from the head group region of lipids by using head-deuterated d-DSPC. Different subphase contrast liquids were used: $H_2O$, $D_2O$ and SMW (Si-matched water). The three water contrasts have scattering length densities $\rho_{H_2O} = -0.56 \times 10^{-6}\,\text{Å}^{-2}$, $\rho_{SMW} = 2.07 \times 10^{-6}\,\text{Å}^{-2}$ and $\rho_{D_2O} = 6.35 \times 10^{-6}\,\text{Å}^{-2}$. With SMW, the Si substrate is "masked" by using a mixture of deuterated and protonated solvent that matches its scattering length. When doing so, the substrate and the solvent are (neutron-) optically indistinguishable, and the actual scattering signal in NR is overwhelmingly due to the deposited lipid bilayers. The spatial resolution of NR allows determining the structural details of adsorbed layers in the Å range. During the experiment, the intensity of the specularly reflected neutron beam (*i.e.* the angle of incident beam $\theta_i$ being equal to angle of the reflected beam $\theta_r$) is recorded relative to the intensity of the incident beam as a function of the component of the wave vector transfer normal to the interface, $Q_z = (4\pi/\lambda)\sin\theta_i$, where $\lambda$ is the neutron wavelength. The resolution of the measurements varied from 1 to 10% ($\Delta Q_z/Q_z$). Measurements were performed on the D17 neutron reflectometer at the ILL [30] in time-of-flight (TOF) mode with a wavelength spread of 2-20 Å at two fixed angles of incidence (0.7° and 3°), thus covering a $Q_z$-range of $0.008\,\text{Å}^{-1}$ to $0.25\,\text{Å}^{-1}$. For higher $Q_z$ the signal is masked by the background noise from the sample.

## 4 Results and discussion

Specular NR experiments provide information about the thickness, composition and rms roughness of thin layers. Reflectivity data were fitted using a box model allowing for sublayers of constant composition specified by the number densities of nuclei of element $i$, $n_i(j)$, determining the scattering length density (SLD) of sublayer $j$, $\rho_j$, via $\rho_j = \sum n_i(j)b_i$ where $b_i$ is the scattering length of species $i$. Each sublayer is assigned a thickness $\Delta_j$ with a roughness, $\sigma$, at each boundary accounting for the smooth composition gradients between the sublayers assuming an error distribution function for the SLD. Each sublayer is characterized by an inner and an outer roughness denoted by $\sigma_j^{\text{in}}$ and $\sigma_j^{\text{out}}$. The model comprises of the following sublayers proceeding from the Si substrate towards the aqueous subphase: i) $SiO_2$ sublayer $\Delta_{SiO_2} = 9 \pm 1$ Å, $\sigma^{\text{in}}_{SiO_2} = 4 \pm 2$ Å and $\sigma^{\text{out}}_{SiO_2} = 2 \pm 1$ Å as determined by analyzing neutron reflectivity data from the bare substrate in two water contrasts; ii) an inner hydrated headgroup sublayer, $j = \text{int}$; iii) a hydrophobic core of lipid hydrocarbon tails $j = \text{tail}$; iv) an exterior hydrated headgroup layer, $j = \text{ext}$. Because of the high hydration level of the PEG chains and their low monomer density, it was not possible to discern this layer and model its features. The SLD of each layer within the box model is $\rho_j = \phi_j\rho_j^0 + (1 - \phi_j)\rho_{\text{solvent}}$, where $\phi_j$ is the volume fraction of $j$, $\rho_j^0$ is the neutron scattering density of the pure $j$ and $\rho_{\text{solvent}}$ is the neutron SLD of the water subphase in contact with the bilayer.

The non-hydrated deuterated DSPC head groups have a $\rho^0_{\text{headgoup}} = 5.7 \times 10^{-6}\,\text{Å}^{-2}$. The SLD of the lipid hydrocarbon tail core region, $\rho^0_{\text{tail}}$ depends on $T$ and the lipid phase reflecting variation of density due to chain fluctuations: $\rho^0_{\text{tail}} = -0.41 \times 10^{-6}\,\text{Å}^{-2}$ in the gel phase comprising closely packed lipids tails.

The pure d-DSPC bilayer was characterized first using $H_2O$ and $D_2O$ and the detailed results thus obtained were used as a reference in subsequent experiments. This allowed for the determination of some of the structural parameters to be used in the later analysis. The proper identification of sublayers is facilitated by the presence of the deuterated head group of the d-DSPC that allows distinguishing between head group and lipid tail regions, especially when measured against pure $H_2O$ subphase. All the PEG containing bilayers were measured in three contrasts, $H_2O$, SMW and $D_2O$ and data were fitted simultaneously. Figure 3 shows an example of the fits in the $H_2O$ contrast and fig. 4 displays the corresponding scattering length density profiles. The fitting procedure was such that initially the parameters of all layers of the bilayers were varied. It was found that the presence of PEG-lipids did not affect the parameters of the water layer and headgroup region adjacent to the silicon substrate. In the final refining these parameters were therefore kept constant at the values of the pure d-DSPC lipid bilayer: inner headgroup layer thickness of $\Delta_{\text{int}} = 9 \pm 2$ Å, water content of $15 \pm 5\%$ and roughness of $\sigma^{\text{in}}_{\text{int}} = \sigma^{\text{out}}_{\text{int}} = 2 \pm 1$ Å; lipid tail region thickness of $\Delta_{\text{tail}} = 41 \pm 2$ Å, water content of

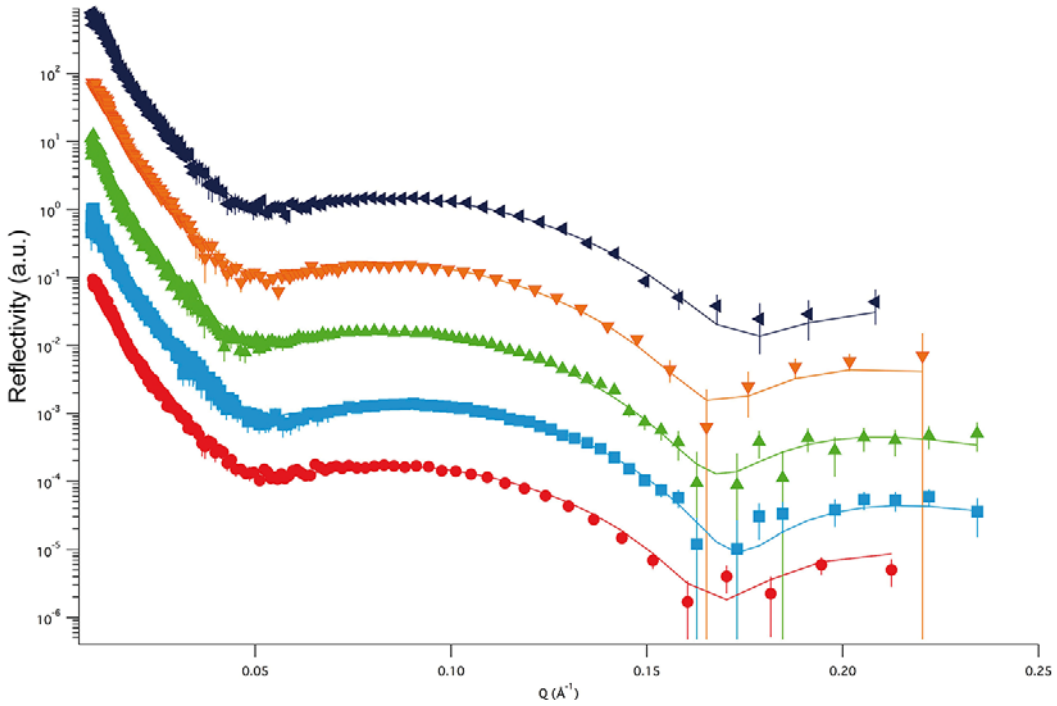


**Fig. 3.** Neutron reflectivity data (points) and fitted lines from adsorbed bilayers with an outer leaflet comprising (red circles) pure d-DSPC $f = 0$, (light blue squares) $N = 16$ at $f = 1.3\%$, (green up-triangles) $N = 16$ at $f = 9\%$, (orange down-triangles) $N = 45$ at $f = 0.35\%$ and (dark blue left-triangles) $N = 45$ at $f = 3.5\%$ in $H_2O$ at 25 °C. Data offset for clarity.

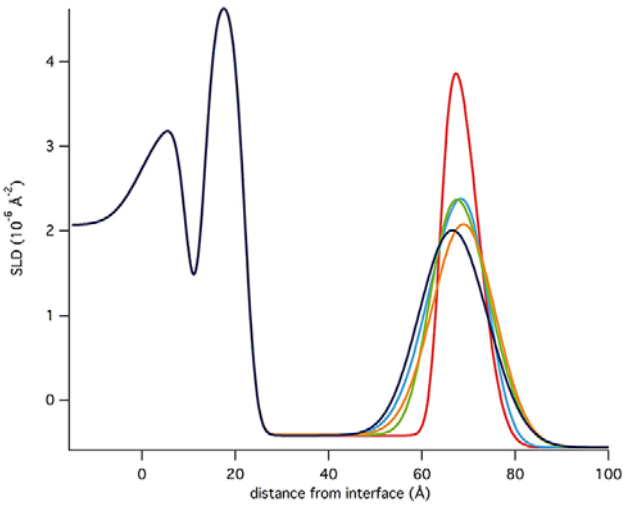


**Fig. 4.** Scattering length density profiles corresponding to the reflectivity data shown in fig. 3 from adsorbed bilayers containing in the outer leaflet of $f = 0$ (red), $N = 16$ at $f = 1.3\%$ (light blue), $N = 16$ at $f = 9\%$ (green) $N = 45$ at $f = 0.35\%$ (orange) and $N = 45$ at $f = 3.5\%$ (dark blue) in $H_2O$ at 25 °C.

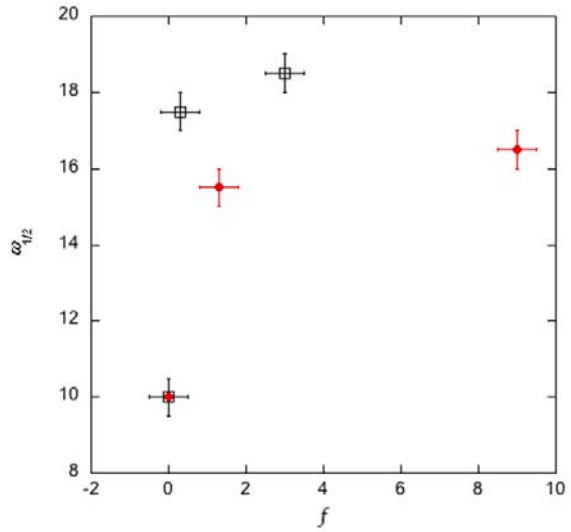


**Fig. 5.** The width at half-height of the SLD profiles, $w_{1/2}$, of the outer headgroup region as a function of PEG-lipid MOLE fraction $f$ for $N = 16$ (circles) and $N = 45$ (squares) samples.

$5 \pm 5\%$. The clear qualitative result is a widening of the outer headgroup region in the presence of PEG, as characterized by $w_{1/2}$ (fig. 5) reflecting contributions due to increased roughness, thickness and water content of this layer (table 1).

The $T$ dependence of the box model parameters obtained from NR was also investigated (data not shown). The biggest effect of the temperature scans on the samples could be attributed to structural modifications induced by the melting of the chains. The resolution of the technique did not permit to draw a clear conclusion regarding the $T$ dependence of the headgroups regions as all changes fell within the error bars. Measurements at room temperature after annealing were consistent with a lower PEG coverage of the bilayer, suggesting desorption of PEG lipids.

**Table 1.** The structural parameters extracted from fitting the outer headgroup data to the box model: thickness, $\Delta_{\rm ext}$, water content, inner and outer roughness, $\sigma_{\rm ext}^{\rm in}$ and $\sigma_{\rm ext}^{\rm out}$, as well as width at half-height, $w_{1/2}$, as extracted from the SLD profile calculated on the basis of these parameters (fig. 5).

| | $f=0$ | $f=1.3\%$ $N=16$ | $f=9\%$ $N=16$ | $f=0.35\%$ $N=45$ | $f=3.5\%$ $N=45$ |
|---|---|---|---|---|---|
| $\Delta_{\rm ext}$ (Å) | $8\pm2$ | $12\pm1$ | $12\pm1$ | $10\pm1$ | $11\pm1$ |
| Water content (%) | $15\pm5$ | $40\pm10$ | $40\pm10$ | $30\pm6$ | $33\pm6$ |
| $\sigma_{\rm ext}^{\rm in}$ (Å) | $2\pm1$ | $6\pm2$ | $4\pm2$ | $6\pm2$ | $6\pm2$ |
| $\sigma_{\rm ext}^{\rm out}$ (Å) | $4\pm2$ | $4\pm1$ | $6\pm1$ | $6\pm1$ | $7\pm1$ |
| $w_{1/2}$ (Å) | $10\pm0.5$ | $15.5\pm0.5$ | $16.5\pm0.5$ | $17.5\pm0.5$ | $18.5\pm0.5$ |

Three results are of importance for distinguishing between the protrusion and the blister models. First, the presence of a water layer adjacent to the solid substrate is necessary to obtain a good model of the reflectivity profiles. Its thickness for all systems is $\Delta_{\rm H_2O}=5\pm1$ Å, as reported earlier for similar systems [22]. The supported lipid bilayer can thus accommodate limited deformation. In particular, this suggests that the supported membrane, as opposed to lipid monolayers on OTS support, could exhibit blisters. A second key point concerns $w_{1/2}$ of the inner headgroup layer. It is independent of $f$ and $N$, being roughly constant at $\approx 10$ Å irrespective of $T$. The third result concerns $w_{1/2}$ of the outer headgroup layers. In contrast to the inner headgroup layer, it increases strongly upon introducing PEG lipids though it exhibits a weak dependence on $f$ for $f\neq0$. Taken together these results support, as discussed earlier, the protrusion hypothesis. The rough approximation, presented in sect. 2, relates $w_{1/2}$ to the $f$ weighted equilibrium height $\langle z\rangle_f=(1-f)z_{\rm free}^{\rm eq}+fz_p^{\rm eq}$, where $z_{\rm free}^{\rm eq}=0$ corresponds to the equilibrium height of a non-functionalized headgroup. It does not allow for the height fluctuations of the simple lipids. These involve only $z>0$ and thus do not average out and lead to an average $\bar{z}_{\rm free}\approx z_p^{\rm eq}$ and similar $T$ dependence for $\bar{z}_{\rm free}$ and $z_p^{\rm eq}$. With this in mind the polymer effect on $w_{1/2}$ may be rationalized by assuming $\bar{z}_{\rm free}/z_p^{\rm eq}=\text{const}'<1$, a point that cannot be distinguished within our rough theoretical description of the protrusions.

## 5 Conclusions

NR on supported membranes with deuterated headgroups provides first direct evidence for polymer-induced stabilization of PEG-lipids protruding out of lipid bilayers. In particular, the results concerning $w_{1/2}$ indicate that terminally anchored PEG chains selectively increase $w_{1/2}$ of the outer headgroup layer with negligible effect on the inner one, as expected for PEG stabilized protrusions. For the particular system studied the results do not support the blisters model where one would expect an increase in $w_{1/2}$ of both layers (fig. 1). These results complement earlier ones, obtained for lipid monolayers, where it was not possible to distinguish between the continuum and molecular models [19,20]. They are of interest because the polymer-induced stabilization of protrusions was invoked to rationalize the enhanced activity of secretory phospholipase $A_2$ (sPLA$_2$) encountering membranes that incorporate PEG lipids. We should emphasize that obtaining direct experimental evidence concerning the protrusion-polymer coupling is challenging because there is little effect on compression force laws and mesoscopic properties such as membrane shape and spontaneous curvature.

The authors wish to thank Ursula Perez-Salas for discussions and for help during the measurements, Ole G. Mouritsen for useful discussions and Priscilla Hardas for a first round of analysis of the data. We thank the ILL for the allocation of beam time and provision of facilities for sample preparation.

## Appendix A. Protrusions within the Alexander model of a brush

In the case of perfectly non-adsorbing surface [27]

$$\frac{Z_a(z,H)}{Z_0}=\frac{1}{2\sqrt{\pi N}a}\left\{\exp\left[-\left(\frac{H-z}{2R_0}\right)^2\right]-\exp\left[-\left(\frac{H+z}{2R_0}\right)^2\right]\right\}, \tag{A.1}$$

leading in the case $z\ll H$ to

$$\frac{Z_a(z,H)}{Z_0}=\frac{1}{2\sqrt{\pi N}a}\frac{Hz}{R_0^2}\exp\left[-\left(\frac{H}{2R_0}\right)^2\right]. \tag{A.2}$$

The elastic free energy of a chain in a brush, $\ln[Z_a(z,H)\,dz/Z_0]$ for $dz=a$, is accordingly

$$\frac{F_{\rm el}}{k_BT}\approx\frac{H^2}{Na^2}-\ln\frac{H}{N^{1/2}a}-\ln\frac{z}{N^{1/2}a}. \tag{A.3}$$

The Alexander model of a brush [24–26] of height $H$ can be thus modified to allow for weak protrusions with $z\ll H$. It now assumes all grafted ends at uniform $z$, free ends straddling the brush boundary at $H$ and a step-like concentration profile with monomer volume fraction $\phi=Na^3/\Sigma H$,

*i.e.* the protrusions affect the elastic free energy but have negligible effect on $\phi$ and the corresponding interaction free energy $F_{\rm int}/k_BT \approx vN^2/H\Sigma$. The total free energy per chain in a brush is thus $F_{\rm brush} = F_{\rm int} + F_{\rm el} + \alpha z$. Its minimization with respect to $z$ and $H$ leads again to $z^p_{\rm eq}$, as given by eq. (3), irrespective of $\Sigma$. The familiar results regarding the equilibrium $H$ are unmodified in this limit. This rough model applies when the equilibrium $F_{\rm int}$ is small in comparison to $\alpha z$ thus avoiding desorption of functionalized lipids.

## References


1. H. Lodish *et al.*, *Molecular Cell Biology* (WH Freeman and Co, New York, 2000).
2. D. Lasic, F. Martin, *Stealth Liposomes* (CRC Press, Boca Raton, FL, 1995).
3. H.E. Warriner, S.H.J. Idziak, N.L. Slack, P. Davidson, C.R. Safinya, Science **27**, 961 (1996).
4. E. Eisenriegler, *Polymers Near Surfaces* (World Scientific, Singapore, 1993).
5. R. Lipowsky, Europhys. Lett. **30**, 197 (1995).
6. M. Breidenich, R.R. Netz, R. Lipowsky, Europhys. Lett. **49**, 431 (2000).
7. T. Bickel, C.M. Marques, C. Jeppesen, Phys. Rev. E **62**, 1124 (2000).
8. T. Bickel, C. Jeppesen, C.M. Marques, Eur. Phys. J. E **4**, 33 (2001).
9. C. Hiergeist, R. Lipowsky, J. Phys. II **6**, 1465 (1996).
10. J.N. Israelachvili, H. Wennerstrom, J. Phys. Chem. **96**, 520 (1992).
11. G.A.E. Aniansson, S.N. Wall, M. Almgren, H. Hoffman, I. Kielmann, W. Ulbricht, R. Zana, J. Lang, C. Tondre, J. Phys. Chem. **80**, 905 (1976).
12. G.A.E. Aniansson, J. Phys. Chem. **82**, 2805 (1978).
13. A. Halperin, O.G. Mouritsen, Eur. Biophys. J. Biophys. Lett. **34**, 967 (2005).
14. R. Lipowsky, S. Grotehans, Europhys. Lett. **23**, 599 (1993).
15. R. Goetz, G. Gompper, R. Lipowsky, Phys. Rev. Lett. **82**, 22 (1999).
16. O.G. Berg, M.H. Gelb, M.-D. Tsai, M.K. Jain, Chem. Rev. **101**, 2613 (2001).
17. D.A. Six, E.A. Dennis, Biochim. Biophys. Acta **1**, 1488 (2000).
18. O.G. Mouritsen, T.L. Andersen, A. Halperin, P.L. Hansen, A.S. Jakobsen, U. Bernchou Jensen, M.O. Jensen, K. Jorgensen, T. Kaasgard, C. Leidy, A. Cohen Simonsen, G.H. Peters, M. Weiss, J. Phys.: Condens. Matter **18**, S1293 (2006).
19. J. Majewski, T.L. Kuhl, M.C. Gerstenberg, J.N. Israelachvili, G.S. Smith, J. Phys. Chem. B **101**, 3122 (1997).
20. J. Majewski, T.L. Kuhl, K. Kjaer, M.C. Gerstenberg, J. Als-Nielsen, J.N. Israelachvili, G.S. Smith, J. Am. Chem. Soc. **120**, 1469 (1998).
21. T.L. Kuhl, J. Majewski, J.Y. Wong, S. Steinberg, D.E. Leckband, J.N. Israelachvili, G.S. Smith, Biophys. J. **75**, 2352 (1998).
22. G. Fragneto, T. Charitat, F. Graner, K. Mecke, L. Perino-Gallice, E. Bellet-Amalric, Europhys. Lett. **53**, 100 (2001).
23. G. Fragneto-Cusani, J. Phys.: Condens. Matter **13**, 4973 (2001).
24. S. Alexander, J. Phys. (Paris) **38**, 977 (1977).
25. S.T. Milner, Science **251**, 905 (1991).
26. A. Halperin, M.V. Tirrell, T.P. Lodge, Adv. Polym. Sci. **100**, 31 (1992).
27. Equation (A.1) is obtained from the $\Gamma \to \infty$ limit of eq. (II-17) of ref. [28]. The $\Gamma \to \infty$ limit corresponds to an impenetrable surface with no adsorption energy.
28. E. Eisenriegler, K. Kremer, K. Binder, J. Chem. Phys. **77**, 6296 (1982).
29. E. Loizou, L. Porcar, P. Schexnailder, G.S. Schmidt, P. Butler, Macromolecules **43**, 1041 (2010).
30. R. Cubitt, G. Fragneto, Appl. Phys. A **74**, 329 (2002).